Hyperon polarization along the beam direction relative to the second and third harmonic event planes in isobar collisions at $\sqrt{s_{NN}} = 200$ GeV

The STAR Collaboration
(Dated: March 17, 2023)

The polarization of Λ and $\bar{\Lambda}$ hyperons along the beam direction has been measured relative to the second and third harmonic event planes in isobar Ru+Ru and Zr+Zr collisions at $\sqrt{s_{NN}} =$ 200 GeV. The second harmonic results follow the emission angle dependence as expected due to elliptic flow, similar to that observed in Au+Au collisions. The polarization relative to the third harmonic event plane, measured for the first time, deviates from zero with 4.8σ significance in 20-60% centrality for $1.1 < p_T < 6.0$ GeV/c and exhibits a similar dependence on the emission angle. These results indicate the formation of a complex vortical structure in the system that follows higher harmonic anisotropic flow originating from the initial density fluctuations. The amplitudes of the sine modulation for the second and third harmonic results are comparable in magnitude, increase from central to peripheral collisions, and show a mild p_T dependence. While the centrality dependence, except in peripheral collisions, is qualitatively consistent with hydrodynamic model calculations including thermal vorticity and shear contributions, the shape of the p_T dependence is very different. Comparison to previous measurements at RHIC and the LHC for the second-order harmonic results shows little dependence on the collision system size and collision energy.

The observation of the Λ hyperon global polarization [1, 2] opens new directions in the study of the dynamics and properties of the matter created in heavy-ion collisions. The global polarization is understood to be a consequence of the partial conversion of the orbital angular momentum of colliding nuclei into the spin angular momentum of produced particles via spin-orbit coupling [3–5] analogous to the Barnett effect [6, 7]. Its observation characterizes the system created in heavy-ion collision as the most vortical fluid known [1]. Recent measurements with Ξ and Ω hyperons [8] confirm the fluid vorticity and global polarization picture of heavy-ion collisions.

In non-central heavy-ion collisions, the initial geometry of the system in the transverse plane has roughly an elliptical shape as depicted in Fig. 1(a). The difference in pressure gradients in the directions of the shorter and longer axes of the ellipse leads to preferential particle emission into the shorter axis, a phenomenon known as elliptic flow. Expansion velocity dependence on the azimuthal angle leads to generation of the vorticity component along the beam direction and therefore particle polarization [9, 10]. Λ hyperon polarization along the beam direction due to elliptic flow was first observed in Au+Au collisions at $\sqrt{s_{NN}} = 200$ GeV by the STAR experiment [11] and later in Pb+Pb collisions at $\sqrt{s_{NN}} =$ 5.02 TeV by the ALICE experiment [12]. Sometimes such polarization driven by anisotropic flow is also referred to as "local polarization" [13, 14].

Various hydrodynamic and transport models [15–20] describe the energy dependence of the global polarization reasonably well. However, most of those models predict the opposite sign for the beam direction component of the polarization, and greatly overpredict its magnitude [10, 14, 21, 22]. Somewhat surprisingly, the data can be very well described by the blast-wave model [23, 24]
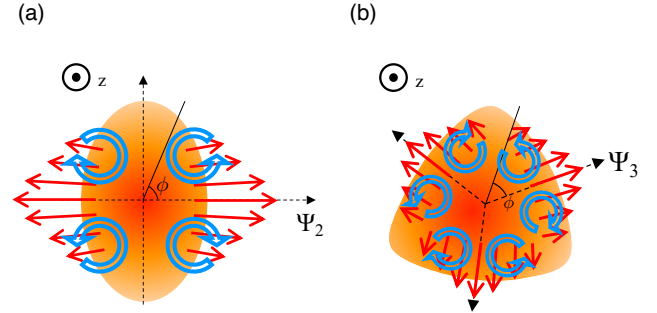

FIG. 1. Sketches illustrating the initial geometry, (a) elliptical shape and (b) triangular shape, viewed from the beam direction in heavy-ion collisions. Solid arrows denote flow velocity indicating stronger collective expansion in the direction of the event plane angle Ψ_n; open arrows indicate vorticities.

using parameters previously determined by the fit to spectra and the HBT radii [11]. The blast-wave model is based on a parameterization of the velocity fields at freeze-out, and the polarization calculations include the contribution only from the kinematic vorticity, neglecting the contributions from the temperature gradient and acceleration. This surprising situation has been dubbed the "spin puzzle" in heavy-ion collisions. It has triggered a series of studies including the calculations based on different types of vorticity [25], the effects of decays from heavier particles [26, 27], and a possible need for a non-equilibrium treatment (see recent review [28] for more details). Most model calculations of the polarization from local vorticity are based on an assumption of local thermal equilibrium of spin degrees of freedom. This may not be the case for the polarization induced by the collective

anisotropic flow that is developed later in time. A new theoretical framework of spin hydrodynamics is under development and is not yet at the level to be compared to experimental data (e.g. see Ref. [29]). Recently, the shear-induced polarization (SIP) was proposed to be included in the calculation of the spin polarization [30, 31]. The contribution from the thermal shear tensor in addition to thermal vorticity helps to describe the experimental data on the local polarization, however it also depends on the implementation details of the shear contributions in the calculation [32, 33]. More experimental data, especially from different systems, are awaited for a better understanding of the local polarization phenomenon and to better constrain theoretical models.

As predicted in Ref. [9], in addition to the elliptic-flow-induced polarization, the higher harmonic flow [34–38], originating mostly from the initial density fluctuations, should also induce local vorticity and polarization similar to those due to elliptic flow. Figure 1(b) depicts a triangular-shape initial condition with vorticity component along the beam direction induced by triangular flow characterized by its reference angle (Ψ_3). Such vorticity, if any, and the resulting polarization would depend on the strength of the anisotropic flow, and the geometrical shape and size of the system at freeze-out [9]. It is of great interest to investigate whether such a complex local vorticity is indeed created in heavy-ion collisions.

In this Letter, we present Λ and $\bar{\Lambda}$ hyperon polarization along the beam direction relative to the second-order event plane, and, for the first time, to the third-order event plane in isobar Ru+Ru and Zr+Zr collisions at $\sqrt{s_{NN}} = 200$ GeV. The high statistics and excellent quality isobar data taken by STAR for the chiral magnetic effect search [39] provide an excellent opportunity for polarization studies in collisions of smaller nuclei compared to Au+Au, as well as to study polarization due to higher harmonic anisotropic flow. The measurements are performed as a function of collision centrality and hyperon transverse momentum. The results are compared to hydrodynamic model calculations as well as to the previous second-order event plane measurements at RHIC and the LHC.

The data of isobar Ru+Ru and Zr+Zr collisions at $\sqrt{s_{NN}} = 200$ GeV were collected in 2018 with the STAR detector. Charged-particle tracks were reconstructed with the time projection chamber (TPC) [40] covering the full azimuth and a pseudorapidity range of $|\eta| < 1$. The collision vertices were reconstructed using the measured charged-particle tracks and were required to be within $(-35, 25)$ cm relative to the TPC center in the beam direction. The asymmetric cut was applied to maximize the statistics since the vertex distribution became asymmetric due to online vertex selection [39]. The vertex in the radial direction relative to the beam center was required to be within 2 cm to reject background from collisions with the beam pipe. Addition-

ally, the difference between the vertex positions along the beam direction from the vertex position detectors (VPD) [41] located at forward and backward pseudorapidities ($4.24 < |\eta| < 5.1$) and that from the TPC was required to be less than 5 cm to suppress pileup events. In order to further suppress the out-of-time pileup events, the events with large difference between the total number of the TPC tracks and the number of the tracks matched with a hit in the time-of-flight (TOF) detector [42] were also removed. Quality assurance based on the event quantities that reflect the detector performance changing with time was performed following the study in Ref. [39]. These selection criteria yielded about 1.8 (2.0) billion minimum bias good events for Ru+Ru (Zr+Zr) collisions, where the minimum bias trigger requires hits of both VPDs. The collision centrality was determined from the measured multiplicity of charged particles within $|\eta| < 0.5$ compared to a Monte Carlo Glauber simulation [39, 43].

The event plane angle Ψ_n was determined by the tracks measured in the TPC, where n denotes the harmonic order. The event plane resolution defined as $\langle\cos[n(\Psi_n^{\mathrm{obs}} - \Psi_n)]\rangle$ [44] ("obs" indicates an observed angle) becomes largest around 10-30% centrality ($\sim$0.62) for the second-order and at 0-5% centrality ($\sim$0.38) for the third-order. Note that the perfect resolution corresponds to 1.0. The resolutions are very similar for the two isobar systems. The event plane detector (EPD) located at forward and backward pseudorapidities ($2.1 < |\eta| < 5.1$) was also used for a cross check of the measurements, which provided consistent results with the TPC event plane measurements. The results presented here utilize the TPC event plane measurements because of its superior resolution compared to the EPD ($\sim$0.38 (0.13) for the second-order (third-order) at the corresponding centralities).

To reconstruct Λ ($\bar{\Lambda}$) hyperons, the decay channel of $\Lambda \to p\pi^-$ ($\bar{\Lambda} \to \bar{p}\pi^+$) was utilized. The daughter charged tracks measured by the TPC were identified using the ionization energy loss in the TPC gas and flight timing information from the TOF detector, and then Λ ($\bar{\Lambda}$) hyperons were reconstructed based on the invariant mass of the two daughters after applying cuts on decay topology to reduce combinatorial background.

Hyperon polarization is studied by utilizing parity-violating weak decays where the daughter baryon emission angle is correlated with the direction of the hyperon spin. The daughter baryon distribution in the hyperon rest frame can be written as:

$$\frac{dN}{d\Omega^*} = \frac{1}{4\pi}(1 + \alpha_H \boldsymbol{P}_H^* \cdot \hat{p}_B^*), \qquad (1)$$

where $d\Omega^*$ is the solid angle element, and $\boldsymbol{P}_H^*$ and $\hat{p}_B^*$ denote hyperon polarization and the unit vector of daughter baryon momentum in the hyperon rest frame (as denoted by an asterisk); α_H is the hyperon decay parameter. The decay parameter α_Λ for the decay $\Lambda \to p + \pi^-$ is set to

$\alpha_\Lambda = 0.732 \pm 0.014$ [45] assuming $\alpha_\Lambda = -\alpha_{\bar\Lambda}$. Polarization along the beam direction P_z [11] is determined as

$$P_z = \frac{\langle \cos\theta_p^* \rangle}{\alpha_H \langle \cos^2\theta_p^* \rangle}, \qquad (2)$$

where θ_p^* is the polar angle of the daughter proton in the Λ rest frame relative to the beam direction. The denominator $\langle \cos^2\theta_p^* \rangle$ accounts for the detector acceptance effect and is found to be close to $1/3$, slightly depending on the hyperon's transverse momentum and centrality.

The systematic uncertainties were evaluated by variation of the topological cuts in the Λ reconstruction $\sim3\%$ (10%), using different methods of the signal extraction as explained below $\sim5\%$ (8%), estimating possible background contribution to the signal $\sim3\%$ (6%), and uncertainty on the decay parameter $\sim2\%$ (2%). The quoted numbers are examples of relative uncertainties for the second-order (third-order) results in 10-30% (0-20%) central collisions. All these contributions were added in quadrature, the value of which was quoted as the final systematic uncertainty. The sine modulation of P_z was extracted by measuring directly $\langle \cos\theta_p^* \sin[n(\phi - \Psi_n)] \rangle$ as a function of the invariant mass. The results were checked by measuring $\langle \cos\theta_p^* \rangle$, corrected for the acceptance effects, as a function of azimuthal angle relative to the event plane, fitting it with the sine Fourier function as presented below in Fig. 2, and followed by correction for the event plane resolution (see Ref. [11] for more details). It should be noted that $\langle \cos\theta_p^* \sin[n(\phi - \Psi_n)] \rangle$ can be directly calculated for a selected mass window if the purity of the Λ samples is high (the background contribution, if any, is negligible). The two approaches provide consistent results. The EPD event plane and different sizes of TPC subevents (see Ref. [11]) were also used for cross checks yielding consistent results as well. Self-correlation effects due to inclusion of the hyperon decay daughters in the TPC event plane determination were studied by excluding the daughters from the event plane calculation and ultimately found to be negligible.

Figure 2 shows $\langle \cos\theta_p^* \rangle^{\mathrm{sub}}$ as a function of Λ ($\bar\Lambda$) azimuthal angle relative to the second- and third-order event planes, where the superscript "sub" represents subtractions of the detector acceptance and inefficiency effects as described in Ref. [11]. Furthermore, the results are multiplied by the sign of α_H for a clearer comparison between Λ and $\bar\Lambda$. The right panel presents the measurement of the longitudinal component of polarization relative to the third-order event plane where sine patterns similar to those in the left panel are clearly seen, indicating the presence of triangular-flow-driven vorticity. Since the results for Λ and $\bar\Lambda$ are consistent with each other, as expected in the vorticity driven polarization picture (note that the difference observed in the third-order results is $\sim1.4\sigma$), both results are combined to enhance the statistical significance.
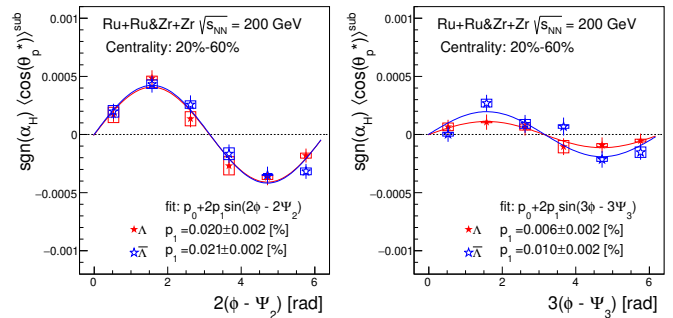

FIG. 2. $\langle \cos\theta_p^* \rangle^{\mathrm{sub}}$ of Λ and $\bar\Lambda$ as a function of hyperon azimuthal angle relative to the second- (left panel) and the third-order (right panel) event planes, $n(\phi - \Psi_n)$, in 20-60% central isobar collisions at $\sqrt{s_{NN}} = 200$ GeV. The sign of the data for $\bar\Lambda$ is flipped as indicated by $\mathrm{sgn}(\alpha_H)$. The solid lines are fit functions used to extract the parameters indicated in the label where p_1 corresponds to the nth-order Fourier sine coefficient. Note that these data are not corrected for the event plane resolution.

The sine modulations of P_z are studied as a function of collision centrality and are presented in Fig. 3. Results of the measurements relative to both event planes are comparable in magnitude and exhibit similar centrality dependence, increasing in more peripheral collisions. Calculations from a hydrodynamic model [33] with shear viscosity $\eta T/(e+P) = 0.08$ and including both the thermal vorticity and shear-induced contributions to the polarization, are in qualitative agreement with the polarization signs and magnitudes. However the centrality dependence, especially in peripheral collisions, is not well described by the model. The model results also depend on a particular implementation of the shear-induced contribution [33]. Note that without the shear-induced polarization contribution the model predicts a polarization with the opposite sign to what is observed in the data. The model calculations within the ideal hydrodynamics scenario (including the shear contribution) leads to almost zero P_z, indicating that the polarization measurements put an additional constraint on the shear viscosity values of the medium [33].

If the observed polarization along the beam direction is induced by collective anisotropic flow, one might naively expect a transverse momentum dependence similar to that of the flow. The P_z sine modulations for measurements relative to both event planes are plotted as a function of hyperons' transverse momentum in Fig. 4. Results show that p_T dependence of the polarization is indeed similar to that of elliptic (v_2) and triangular (v_3) flow. While the third-order P_z modulation is smaller than the second-order for $p_T < 1.5$ GeV/c, the third-order results seem to increase faster, with a hint of out-pacing the second-order results at $p_T > 2$ GeV/c. The significance of the third-order results away from zero is 4.8σ
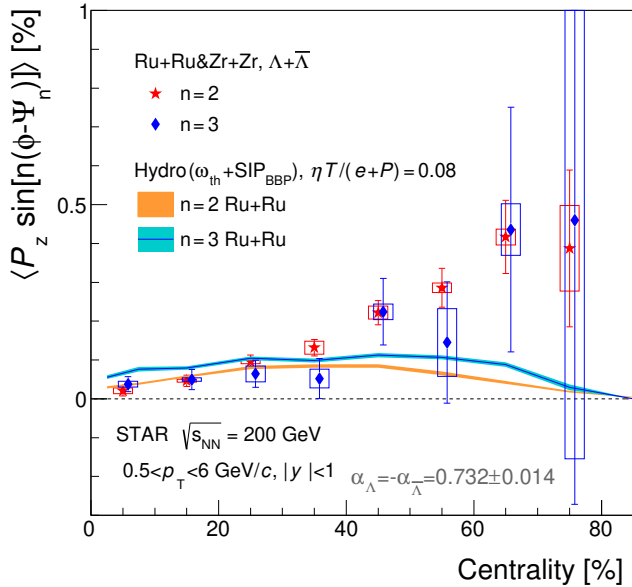
FIG. 3. Centrality dependence of the second- and the third-order Fourier sine coefficients of $\Lambda + \bar{\Lambda}$ polarization along the beam direction in isobar Ru+Ru and Zr+Zr collisions at $\sqrt{s_{NN}} = 200$ GeV. Open boxes show systematic uncertainties. Solid bands show calculations from hydrodynamic model including contribution from the shear-induced polarization based on Ref. [46] (noted as "SIP$_{\mathrm{BBP}}$") in addition to that due to thermal vorticity ω_{th} [33].
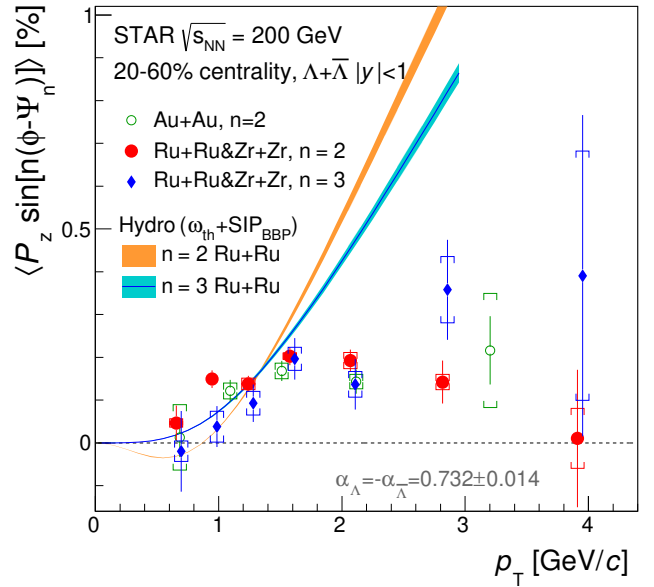
FIG. 4. Transverse momentum dependence of the second-and third-order Fourier sine coefficients of $\Lambda + \bar{\Lambda}$ polarization along the beam direction for 20-60% central isobar Ru+Ru and Zr+Zr collisions at $\sqrt{s_{NN}} = 200$ GeV, compared to the second-order measurements in Au+Au collisions [11]. Open boxes show systematic uncertainties. The results for the third-order event plane measurements in isobar collisions are slightly shifted for a better visibility. Solid bands present calculations from the hydrodynamic model [33] (see Fig. 3 caption).

for $1.1 < p_T < 6.0$ GeV/c considering statistical and systematic uncertainties in quadrature. A similar pattern is also observed in the flow measurements [47, 48] which further supports that the observed polarization is driven by collective flow. The hydrodynamic model calculations exhibit stronger p_T dependence than that in the data and predict smaller values of the second-order polarization compared to the third-order at low p_T. In the model, such behavior is determined by two competing mechanisms, the thermal vorticity and the shear-induced polarization. The second-order polarization results for isobar collisions are found to be comparable to or slightly higher than those for Au+Au collisions.

Figure 5 shows the centrality dependence of the second sine Fourier coefficients of P_z in isobar collisions compared to results from Au+Au collisions at $\sqrt{s_{NN}} = 200$ GeV [11] and Pb+Pb collisions at $\sqrt{s_{NN}} = 5.02$ TeV from the ALICE experiment [12]. The results do not show any strong energy dependence nor system size dependence for a given centrality. The isobar collisions, a smaller system compared to Au+Au, show slightly larger polarization values in midcentral collisions, but the difference is not significant. Note that the elliptic flow v_2 in 5.02 TeV Pb+Pb collisions [49] is ~60% larger than that in 200 GeV isobar collisions [39]. The data do not follow a naive expectation from the v_2 magnitude, i.e., larger

local polarization in Pb+Pb for a given centrality. The data are also plotted as a function of an average number of nucleon participants N_{part} estimated from the Glauber model in the inset of Fig. 5, showing that the data scales better with N_{part}, indicating a possible importance of the system size in vorticity formation.

In conclusion, Λ and $\bar{\Lambda}$ hyperon polarization along the beam direction has been measured in isobar Ru+Ru and Zr+Zr collisions at $\sqrt{s_{NN}} = 200$ GeV, with respect to the second-order event plane and, for the first time, to the third-order event plane. The polarization is found to have a sinusoidal azimuthal dependence relative to both the event planes, indicating the creation of complex vorticities induced by the elliptic and triangular flow in heavy-ion collisions. The second- and third-order sine Fourier coefficients of the polarization exhibit increasing trends toward peripheral collisions and a mild p_T dependence. Hydrodynamic model calculations including both thermal vorticity and thermal shear contributions qualitatively describe the data with the correct sign for both harmonics though the model underestimates the data in peripheral collisions and predict different shape of the p_T dependence. The polarization also exhibits p_T dependence similar to those of elliptic and triangular flow
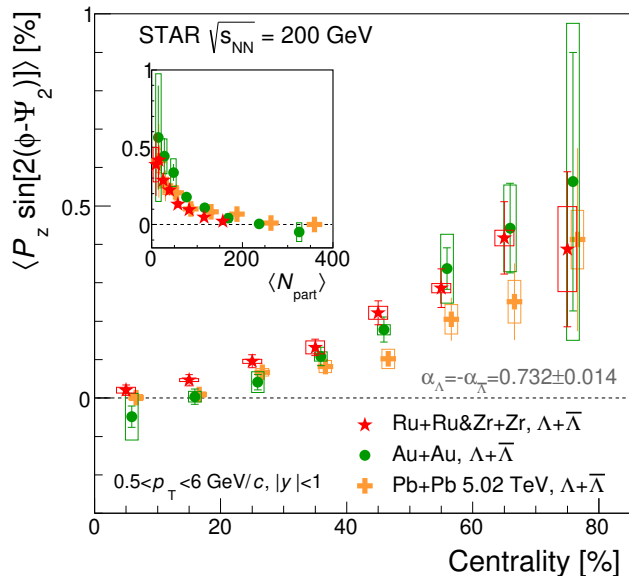
FIG. 5. Comparison of the second Fourier sine coefficients of $\Lambda + \bar\Lambda$ polarization component along the beam direction among isobar and Au+Au collisions at $\sqrt{s_{NN}} = 200$ GeV [11] and Pb+Pb collisions at $\sqrt{s_{NN}} = 5.02$ TeV [12] as a function of centrality. Open boxes show systematic uncertainties. The inset presents the same data plotted as a function of average number of participants $\langle N_{\text{part}} \rangle$. Note that the data points for Pb+Pb collisions are rescaled to account for the difference in the decay parameter α_Λ used in Pb+Pb analysis.

coefficients. The second-order sine coefficient is also compared to those in 200 GeV Au+Au and 5.02 TeV Pb+Pb collisions, showing little system size dependence and energy dependence of the polarization. These results provide new insights into polarization mechanism and vorticity fields in heavy-ion collisions as well as additional constraints on properties and dynamics of the matter created in the collisions.

[1] L. Adamczyk et al. (STAR), "Global Λ hyperon polarization in nuclear collisions: evidence for the most vortical fluid," Nature 548, 62–65 (2017), arXiv:1701.06657 [nucl-ex].
[2] J. Adam et al. (STAR Collaboration), "Global polarization of Λ hyperons in Au+Au collisions at $\sqrt{s_{NN}} = 200$ GeV," Phys. Rev. C 98, 014910 (2018).
[3] Z.-T. Liang and X.-N. Wang, "Globally polarized quark-gluon plasma in non-central A+A collisions," Phys. Rev. Lett. 94, 102301 (2005), [Erratum: Phys.Rev.Lett. 96, 039901 (2006)], arXiv:nucl-th/0410079.
[4] S. A. Voloshin, "Polarized secondary particles in unpolarized high energy hadron-hadron collisions?" (2004), arXiv:nucl-th/0410089 [nucl-th].
[5] F. Becattini, F. Piccinini, and J. Rizzo, "Angular momentum conservation in heavy ion collisions at very high energy," Phys. Rev. C 77, 024906 (2008), arXiv:0711.1253 [nucl-th].
[6] S. J. Barnett, "Magnetization by rotation," Phys. Rev. 6, 239–270 (1915).
[7] S. J. Barnett, "Gyromagnetic and electron-inertia effects," Rev. Mod. Phys. 7, 129 (1935).
[8] Jaroslav Adam et al. (STAR), "Global Polarization of Ξ and Ω Hyperons in Au+Au Collisions at $\sqrt{s_{NN}}$ = 200 GeV," Phys. Rev. Lett. 126, 162301 (2021), arXiv:2012.13601 [nucl-ex].
[9] S. A. Voloshin, "Vorticity and particle polarization in heavy ion collisions (experimental perspective)," 17th International Conference on Strangeness in Quark Matter (SQM 2017) Utrecht, the Netherlands, July 10-15, 2017, (2017), 10.1051/epjconf/201817107002, [EPJ Web Conf.17,10700(2018)].
[10] F. Becattini and Iu. Karpenko, "Collective longitudinal polarization in relativistic heavy-ion collisions at very high energy," Phys. Rev. Lett. 120, 012302 (2018).
[11] Jaroslav Adam et al. (STAR), "Polarization of Λ (Λ̄) hyperons along the beam direction in Au+Au collisions at $\sqrt{s_{NN}} = 200$ GeV," Phys. Rev. Lett. 123, 132301 (2019), arXiv:1905.11917 [nucl-ex].
[12] Shreyasi Acharya et al. (ALICE), "Polarization of Λ and Λ̄ Hyperons along the Beam Direction in Pb-Pb Collisions at $\sqrt{s_{NN}}$=5.02 TeV," Phys. Rev. Lett. 128, 172005 (2022), arXiv:2107.11183 [nucl-ex].
[13] Jian-Hua Gao, Zuo-Tang Liang, Shi Pu, Qun Wang, and Xin-Nian Wang, "Chiral Anomaly and Local Polarization Effect from Quantum Kinetic Approach," Phys. Rev. Lett. 109, 232301 (2012), arXiv:1203.0725 [hep-ph].
[14] X.-L. Xia, H. Li, Z.-B. Tang, and Q. Wang, "Probing vorticity structure in heavy-ion collisions by local Λ polarization," Phys. Rev. C 98, 024905 (2018).
[15] I. Karpenko and F. Becattini, "Study of Λ polarization in

relativistic nuclear collisions at $\sqrt{s_{NN}} = 7.7$ –200 GeV," Eur. Phys. J. C **77**, 213 (2017), arXiv:1610.04717 [nucl-th].

[16] Hui Li, Long-Gang Pang, Qun Wang, and Xiao-Liang Xia, "Global Λ polarization in heavy-ion collisions from a transport model," Phys. Rev. C **96**, 054908 (2017), arXiv:1704.01507 [nucl-th].

[17] Y. Sun and C. M. Ko, "Λ hyperon polarization in relativistic heavy ion collisions from a chiral kinetic approach," Phys. Rev. C **96**, 024906 (2017).

[18] Y. Xie, D. Wang, and L. P. Csernai, "Global Λ polarization in high energy collisions," Phys. Rev. C **95**, 031901 (2017).

[19] Y. B. Ivanov, V. D. Toneev, and A. A. Soldatov, "Estimates of hyperon polarization in heavy-ion collisions at collision energies $\sqrt{s_{NN}} = 4$–40 GeV," Phys. Rev. C **100**, 014908 (2019), arXiv:1903.05455 [nucl-th].

[20] O. Vitiuk, L. V. Bravina, and E. E. Zabrodin, "Is different Λ and $\bar{\Lambda}$ polarization caused by different spatio-temporal freeze-out picture?" Phys. Lett. B **803**, 135298 (2020), arXiv:1910.06292 [hep-ph].

[21] Baochi Fu, Kai Xu, Xu-Guang Huang, and Huichao Song, "Hydrodynamic study of hyperon spin polarization in relativistic heavy ion collisions," Phys. Rev. C **103**, 024903 (2021), arXiv:2011.03740 [nucl-th].

[22] Wojciech Florkowski, Avdhesh Kumar, Radoslaw Ryblewski, and Aleksas Mazeliauskas, "Longitudinal spin polarization in a thermal model," Phys. Rev. C **100**, 054907 (2019), arXiv:1904.00002 [nucl-th].

[23] E. Schnedermann, J. Sollfrank, and U. W. Heinz, "Thermal phenomenology of hadrons from $200A$ GeV S+S collisions," Phys. Rev. C **48**, 2462 (1993).

[24] F. Retiere and M. A. Lisa, "Observable implications of geometrical and dynamical aspects of freeze-out in heavy ion collisions," Phys. Rev. C **70**, 044907 (2004).

[25] Hong-Zhong Wu, Long-Gang Pang, Xu-Guang Huang, and Qun Wang, "Local spin polarization in high energy heavy ion collisions," Phys. Rev. Research. **1**, 033058 (2019), arXiv:1906.09385 [nucl-th].

[26] Francesco Becattini, Gaoqing Cao, and Enrico Speranza, "Polarization transfer in hyperon decays and its effect in relativistic nuclear collisions," Eur. Phys. J. C **79**, 741 (2019), arXiv:1905.03123 [nucl-th].

[27] Xiao-Liang Xia, Hui Li, Xu-Guang Huang, and Huan Zhong Huang, "Feed-down effect on Λ spin polarization," Phys. Rev. C **100**, 014913 (2019), arXiv:1905.03120 [nucl-th].

[28] F. Becattini and M. A. Lisa, "Polarization and Vorticity in the Quark Gluon Plasma," Annual Review of Nuclear and Particle Science **70**, 395–423 (2020), arXiv:2003.03640 [nucl-ex].

[29] Wojciech Florkowski, Avdhesh Kumar, and Radoslaw Ryblewski, "Relativistic hydrodynamics for spin-polarized fluids," Prog. Part. Nucl. Phys. **108**, 103709 (2019), arXiv:1811.04409 [nucl-th].

[30] Baochi Fu, Shuai Y. F. Liu, Longgang Pang, Huichao Song, and Yi Yin, "Shear-Induced Spin Polarization in Heavy-Ion Collisions," Phys. Rev. Lett. **127**, 142301 (2021), arXiv:2103.10403 [hep-ph].

[31] F. Becattini, M. Buzzegoli, G. Inghirami, I. Karpenko, and A. Palermo, "Local Polarization and Isothermal Local Equilibrium in Relativistic Heavy Ion Collisions," Phys. Rev. Lett. **127**, 272302 (2021), arXiv:2103.14621 [nucl-th].

[32] Wojciech Florkowski, Avdhesh Kumar, Aleksas Mazeliauskas, and Radoslaw Ryblewski, "Effect of thermal shear on longitudinal spin polarization in a thermal model," Phys. Rev. C **105**, 064901 (2022), arXiv:2112.02799 [hep-ph].

[33] Sahr Alzhrani, Sangwook Ryu, and Chun Shen, "Λ spin polarization in event-by-event relativistic heavy-ion collisions," Phys. Rev. C **106**, 014905 (2022), arXiv:2203.15718 [nucl-th].

[34] A. Adare et al. (PHENIX), "Measurements of Higher-Order Flow Harmonics in Au+Au Collisions at $\sqrt{s_{NN}} = 200$ GeV," Phys. Rev. Lett. **107**, 252301 (2011), arXiv:1105.3928 [nucl-ex].

[35] K. Aamodt et al. (ALICE), "Higher harmonic anisotropic flow measurements of charged particles in Pb-Pb collisions at $\sqrt{s_{NN}}$=2.76 TeV," Phys. Rev. Lett. **107**, 032301 (2011), arXiv:1105.3865 [nucl-ex].

[36] Georges Aad et al. (ATLAS), "Measurement of the azimuthal anisotropy for charged particle production in $\sqrt{s_{NN}} = 2.76$ TeV lead-lead collisions with the ATLAS detector," Phys. Rev. C **86**, 014907 (2012), arXiv:1203.3087 [hep-ex].

[37] Serguei Chatrchyan et al. (CMS), "Centrality dependence of dihadron correlations and azimuthal anisotropy harmonics in PbPb collisions at $\sqrt{s_{NN}} = 2.76$ TeV," Eur. Phys. J. C **72**, 2012 (2012), arXiv:1201.3158 [nucl-ex].

[38] L. Adamczyk et al. (STAR), "Third Harmonic Flow of Charged Particles in Au+Au Collisions at sqrtsNN = 200 GeV," Phys. Rev. C **88**, 014904 (2013), arXiv:1301.2187 [nucl-ex].

[39] Mohamed Abdallah et al. (STAR), "Search for the chiral magnetic effect with isobar collisions at $\sqrt{s_{NN}}$=200 GeV by the STAR Collaboration at the BNL Relativistic Heavy Ion Collider," Phys. Rev. C **105**, 014901 (2022), arXiv:2109.00131 [nucl-ex].

[40] M. Anderson et al., "The STAR time projection chamber: A unique tool for studying high multiplicity events at RHIC," Nucl. Instrum. Meth. A **499**, 659 (2003).

[41] W. J. Llope et al., "The STAR Vertex Position Detector," Nucl. Instrum. Meth. A **759**, 23 (2014).

[42] W. J. Llope, "Multigap RPCs in the STAR experiment at RHIC," Nucl. Instrum. Meth. A **661**, S110 (2012).

[43] M. L. Miller, K. Reygers, S. J. Sanders, and P. Steinberg, "Glauber modeling in high-energy nuclear collisions," Ann. Rev. Nucl. Part. Sci. **57**, 205 (2007).

[44] A. M. Poskanzer and S. A. Voloshin, "Methods for analyzing anisotropic flow in relativistic nuclear collisions," Phys. Rev. C **58**, 1671 (1998).

[45] P.A. Zyla et al. (Particle Data Group), "Review of Particle Physics," PTEP **2020** issue 8, 083C01 (2020).

[46] F. Becattini, M. Buzzegoli, and A. Palermo, "Spin-thermal shear coupling in a relativistic fluid," Phys. Lett. B **820**, 136519 (2021), arXiv:2103.10917 [nucl-th].

[47] Jaroslav Adam et al. (ALICE), "Higher harmonic flow coefficients of identified hadrons in Pb-Pb collisions at $\sqrt{s_{NN}} = 2.76$ TeV," JHEP **09**, 164 (2016), arXiv:1606.06057 [nucl-ex].

[48] A. Adare et al. (PHENIX), "Measurement of the higher-order anisotropic flow coefficients for identified hadrons in Au+Au collisions at $\sqrt{s_{NN}} = 200$ GeV," Phys. Rev. C **93**, 051902 (2016), arXiv:1412.1038 [nucl-ex].

[49] Jaroslav Adam et al. (ALICE), "Anisotropic flow of charged particles in Pb-Pb collisions at $\sqrt{s_{NN}} = 5.02$ TeV," Phys. Rev. Lett. **116**, 132302 (2016),

arXiv:1602.01119 [nucl-ex].